Int. J. Cancer: **119,** 839–846 (2006)
© 2006 Wiley-Liss, Inc.

Production of VEGF165 by Ewing's sarcoma cells induces vasculogenesis and the incorporation of $CD34^+$ stem cells into the expanding tumor vasculature

Tim H. Lee[1], Marcela F. Bolontrade[1], Laura L. Worth[1], Hui Guan[1], Lee M. Ellis[2] and Eugenie S. Kleinerman[1]*

[1]*Division of Pediatrics, University of Texas, MD Anderson Cancer Center, Houston, TX, USA*
[2]*Department of Surgical Oncology, University of Texas, MD Anderson Cancer Center, Houston, TX, USA*

The Ewing's sarcoma cell line TC71 overexpresses vascular endothelial growth factor isoform 165 ($VEGF_{165}$), a potent proangiogenic molecule that induces endothelial cell proliferation, migration, and chemotaxis. $CD34^+$ bone marrow stem cells can differentiate into endothelial and hematopoietic cells. We used a transplant model to determine whether $CD34^+$ cells migrate from the bone marrow to Ewing's sarcoma tumors and participate in the neovascularization process that supports tumor growth. We also examined the role of $VEGF_{165}$ in $CD34^+$ cell migration. Human umbilical cord $CD34^+$ cells were transplanted into sublethally irradiated severe combined immunodeficient mice. Seven days later, the mice were injected subcutaneously with TC71 tumor cells. Tumors were excised 2 weeks later and analyzed by immunohistochemistry. The tumor sections expressed both human VE-cadherin and mouse CD31, indicating involvement of donor-derived human cells in the tumor vessels. To determine the role of $VEGF_{165}$ in the chemoattraction of $CD34^+$ cells, we generated two $VEGF_{165}$-deficient TC71 clones, a stable anti-sense $VEGF_{165}$ cell line (Clone 17) and a $VEGF_{165}$ siRNA-inhibited clone (TC/si$VEGF_{7\text{-}1}$). The resulting $VEGF_{165}$-deficient tumor cells had normal growth rates *in vitro*, but had delayed growth when implanted into mice. Immunohistochemical analysis revealed decreased infiltration of $CD34^+$ cells into both $VEGF_{165}$-deficient tumors. These data show that bone marrow stem cells contribute to the growing tumor vasculature in Ewing's sarcoma and that $VEGF_{165}$ is critical for the migration of $CD34^+$ cells from the bone marrow into the tumor.
© *2006 Wiley-Liss, Inc.*

Key words: Ewing's sarcoma; vasculogenesis; $CD34^+$ cell; vascular endothelial growth factor

The Ewing's sarcoma family of tumors (ESFT) consists of highly vascular and hemorrhagic soft tissue neoplasms of neuroectodermal origin.[1] The majority of these tumors (but not all) are characterized by a unique chromosomal translocation between the *EWS* gene on chromosome 22 and the *FLI1* gene on chromosome 11.[2] Greater than 95% of ESFTs harbor either the *EWS*/*FLI1* or *EWS*/*ERG* translocations.[3] Thus, detection of an *EWS*/*ETS* fusion gene is pathognomonic for Ewing's sarcoma.[3] Combining chemotherapy with surgery and/or radiotherapy has increased the 2-year disease-free survival rate from 15% to 40–60% for patients with no detectable metastases at diagnosis. In patients with detectable metastases, the long-term survival rate is only 20–25%.[4] Unfortunately, these survival rates have remained stagnant for the past 15 years. Understanding the biology of tumor growth may identify new therapeutic approaches.

Vascular endothelial growth factor (VEGF) has a central role in normal angiogenesis and vasculogenesis. When applied to confluent microvascular endothelial cells, VEGF induces their invasion into collagen gels to form capillary-like structures.[5] Because of its potent angiogenic effects, dysregulation of VEGF is a major factor contributing to the pathogenesis of a variety of diseases, including macular degeneration, rheumatoid arthritis, and tumor growth.[6] Analysis of patient samples has revealed elevated VEGF levels in several different tumors.[7–9] VEGF expression by tumors and increased levels of VEGF in the serum of breast cancer patients and in the ovarian cyst fluid of ovarian cancer patients are associated with increased microvessel density within tumors and poor outcomes.[10,11] The inhibition or overexpression of VEGF in glioblastoma and colon carcinoma affects tumor angiogenicity, tumorigenicity, and metastasis.[12–14]

The progression of rapidly growing tumors such as Ewing's sarcoma, a hemorrhagic soft tissue neoplasm of neuroectodermal origin, depends on the induction of blood vessel formation to support this growth. Given the highly vascular nature of Ewing's sarcoma tumors, it is not surprising to find that VEGF is overexpressed in several different Ewing's sarcoma cell lines[15] and is elevated in 55% of Ewing's sarcoma tumors.[16] The proangiogenic influence of VEGF is mediated in part by its potency as an activator and chemoattractant for mature and progenitor endothelial cells.

Endothelial progenitor cells from the bone marrow have been shown to migrate to and incorporate into areas of physiological and pathological neovascularization to form new blood vessels.[17] Studies using ischemic limb models have demonstrated the ability of $CD34^+$ stem cells from bone marrow to differentiate into endothelial progenitor cells and participate in neoangiogenesis.[18,19] Our previous investigations showed that Ewing's tumors recruit bone marrow derived progenitor cells to participate in tumor neoangiogenesis.[20] The present study demonstrates that, similar to our findings with whole bone marrow cells, $CD34^+$ cells migrate to the tumor vascular bed. We further demonstrated that the growth of Ewing's tumors depends on $VEGF_{165}$, a specific isoform that is secreted rather than membrane bound $VEGF_{189}$. Inhibition of $VEGF_{165}$ reduced the migration of stem cells into the growing tumor, decreased tumor vessel expansion, and inhibited tumor growth.

Material and methods

Isolation of $CD34^+$ stem cells

Human umbilical cord blood from the St. Louis Cord Blood Bank (St. Louis, MO) was washed twice by diluting with warmed Dulbecco's PBS and then centrifuged for 10 min at 1,500 rpm. Mononuclear layer cells were separated using Histopaque-1077 (Sigma Diagnostics, St. Louis, MO), washed, and resuspended at a concentration of 2–8 $\times$ 10^7 cells/ml in Dulbecco's PBS with 2% fetal bovine serum. Enrichment of $CD34^+$ cells was done with a StemSep progenitor cell separation kit (StemCell Technologies, Vancouver, British Columbia). Mononuclear layer cells and purified $CD34^+$ stem cells were analyzed by fluorescence-activated cytometric analysis using R-phycoerythrin-conjugated mouse anti-human CD34 (8G12; BD PharMingen, San Diego, CA), fluorescein isothiocyanate-conjugated mouse anti-human CD45 (H130; BD PharMingen), purified mouse anti-human vascular endothelial cadherin (VEC; Chemicon International, Temecula, CA), and purified mouse anti-human leukocyte antigen (HLA-) A, B, and HLA-C (BD PharMingen) antibodies. Isotypic mouse $IgG_1\kappa$ antibodies conjugated to either R-phycoerytherin or fluorescein isothiocyanate were used as negative controls (BD PharMingen). Fluorescein isothiocyanate-conjugated rat anti-mouse $IgG_1\kappa$ secondary antibody (BD PharMingen) was used with samples stained with

Grant sponsor: NIH; Grant numbers: R01 CA103986, CA16672; Grant sponsor: Kayton Fund.
***Correspondence to:** Division of Pediatrics, University of Texas, MD Anderson Cancer Center, 1515 Holcombe Boulevard, Unit 87, Houston, TX 77030, USA. Fax: 713-794-5042. E-mail: ekleiner@mdanderson.org
Received 2 December 2005; Accepted 24 December 2005
DOI 10.1002/ijc.21916
Published online 23 March 2006 in Wiley InterScience (www.interscience.wiley.com).

purified primary antibodies. $CD34^+$ cells were cultured at 37°C in Stem Pro-34 medium (Invitrogen, Carlsbad, CA) supplemented with Stem Span CC100 cytokine cocktail (Stem Cell Technologies).

Transplantation

Six-week-old nonobese diabetic/severe combined immunodeficient (NOD/SCID) mice (Jackson Laboratories, Bar Harbor, ME) were used in our human $CD34^+$ cell transplantation model based on previous reports demonstrating the consistent engraftment of these stem cells into SCID mice bone marrow with subsequent maintenance of a proliferating primitive human bone marrow cell population.[21] The mice underwent sublethal whole-body irradiation with 350 cGy using an external cesium source (^{137}Cs Mark 1 irradiator; J. L. Shepherd & Associates, Glendale, CA). All experiments were approved by the Institutional Animal Care and Use committee of the University of Texas M. D. Anderson Cancer Center. Within 2 hr after irradiation, between 1×10^4 and 1×10^5 human $CD34^+$ cells were injected into the tail veins of the mice. The mice were then given acid-water (pH 2–3) plus neomycin (2 g/l, by mouth; Sigma) for 1 week after transplantation. Engraftment was confirmed 7 days after transplantation by immunohistochemical detection of human HLA-A, HLA-B, and HLA-C.

Implantation of Ewing's sarcoma tumor cells and Matrigel

TC71 human Ewing's sarcoma cells were maintained as previously described.[15,20] Growth factor-depleted Matrigel basement membrane alone (300 μl; BD Bioscience, San Diego, CA), Matrigel with recombinant human VEGF (100 ng/ml; Sigma), or Matrigel with 2×10^6 TC71 cells was injected subcutaneously on the ventral side of NOD/SCID mice 1 week after transplantation with human $CD34^+$ cells. For *in vivo* $CD34^+$ cell migration experiments, 7 mice were used per experimental group. Matrigel plugs containing tumor cells were injected into each mouse and allowed to grow *in vivo* for 2 weeks. The mice were killed 3 weeks after stem cell transplantation (14 days after Matrigel injection). The Matrigel plugs were excised, placed in optimal cutting temperature compound (Sakura Finetek USA, Torrance, CA), snap-frozen in liquid nitrogen, and stored at −80°C.

Immunohistochemistry

Bone marrow cells from NOD/SCID mice previously transplanted with human $CD34^+$ cells were isolated by flushing the hind femurs of the mice. Samples were plated on poly-L-lysine coated microscope slides. Samples were allowed to attach to slides for 6 hr and then fixed in cold acetone for 10 min. Endogenous peroxidase was blocked using 3% H_2O_2 in PBS. To block nonspecific binding of secondary anti-mouse IgG, protein block solution (1% normal goat serum and 5% normal horse serum in PBS) and goat anti-mouse F(ab) fragment (Jackson ImmunoResearch, West Grove, PA) were applied to samples and incubated for 3 hr at room temperature or for 18 hr at 4°C. The samples were then protein-blocked again without F(ab) fragments for 20 min at room temperature. Expression of human HLA was detected by using mouse anti-human HLA antibody (BD PharMingen), rat anti-mouse incubating samples with peroxidase antibody (Jackson ImmunoResearch), and the chromogen diaminobenzidine.

For detection of human VEC, mouse platelet-endothelial cell adhesion molecule (mCD31), and green fluorescent protein, frozen tissue sections were fixed in acetone, blocked using 4% fish gelatin in PBS, and incubated with mouse anti-human VEC (Chemicon International), rat anti-mCD31 (MEC 13.3; BD PharMingen), or rabbit anti-green fluorescent protein (Santa Cruz Biotechnology, Santa Cruz, CA). When using mouse monoclonal antibodies, slides were preblocked overnight with F(ab) fragment (Jackson ImmunoResearch) and then incubated with rat anti-mouse Alexa Fluor 594, goat anti-rabbit Alexa Fluor 594, goat anti-rabbit Alexa Fluor 488, or goat anti-rat Alexa Fluor 488 (Molecular Probes, Eugene, OR) as secondary antibodies. Hoescht 33342 dye (Molecular Probes) was used to stain cell nuclei.

Fluorescent images were captured at 10× (eyepiece) and 10× (objective) with Optimas imaging software (San Diego, CA) and saved as 32 bit TIF files. The digital image files were analyzed using Scion imaging software (Frederick, MD). The number of positive pixels in each viewing field was used to quantify the CD31-positive or human VEC-positive cells within that tumor area. For *in vivo* human $CD34^+$ cell migration experiments: 33, 35, and 24 viewing fields for TC71, clone 17, and TC71-neo tumors were analyzed, respectively. The mean number of positive pixels per viewing field were compared and analyzed.

For confocal microscopy, goat anti-rat Cy5-conjugated IgG (H+L) and goat anti-mouse Cy3-conjugated $F(ab')_2$ fragment (Jackson ImmunoResearch) were used as the secondary antibodies. Sytox Green (Molecular Probes) was used to stain cell nuclei.

Antisense $VEGF_{165}$TC71 clone

A pCDNA 3.0 plasmid with the 604 bp full-length cDNA encoding $VEGF_{165}$ was cloned in the antisense direction and transfected into 1×10^6 TC71 cells using Fugene 6 (Roche Diagnostics, Indianapolis, IN). The cells were expanded and placed in selection medium [Eagle's minimal essential medium with 500 μg/ml G418 (Invitrogen)]. Ninety six resistant colonies were isolated and cultured in selection medium for 30 days. Thirty three colonies were analyzed by reverse transcribed polymerase chain reaction (RT-PCR) and enzyme-linked immunosorbent assay (ELISA; R&D Systems, Minneapolis, MN) for expression of antisense $VEGF_{165}$ mRNA and $VEGF_{165}$ protein production.

RT-PCR and strand-specific RT-PCR

Total mRNA was purified using Trizol reagent (Invitrogen). Nonspecific reverse transcriptase reaction with the Reverse transcriptase system (Promega, Madison, WI) was performed using $oligo(dT)_{15}$ primers. For strand-specific RT-PCR, purified mRNA was treated with DNA-free DNA treatment and removal agent (Ambion, Austin, TX), and either a sense or an antisense DNA primer for VEGF was used in the reverse transcriptase reaction. The first pair of primers flanked exons 4 and 8 and had a predicted product length of 228 bp. The sequences of the primers were: 5′-CACATAGGAGAGATGAGCTTC-3′ (sense; VEGF1) and 5′-CCG-CCTCGGCTTGTCACAT-3′ (antisense; VEGF2). The second pair flanked exons 1 and 4 and had a predicted product length of 352 bp. The sequences of the primers were: 5′-TTCTGCTGTCTTGGGTGC-ATTGG-3′ (sense; VEGF3) and 5′-TCTCTCCTATGTGCTGGC-CTT-3′ (antisense; VEGF4). PCR reactions were performed using a PTC-200 Peltier thermocycler (MJ Research, Reno, NV). For primers VEGF1 and VEGF2, DNA was denatured for 3 min at 95°C and then cycled 28 times at 95°C for 10 sec, 62°C for 30 sec, and 72°C for 45 sec. Finally, the reaction was held at 72°C for 10 min. Samples were maintained at 4°C until analysis. For primers VEGF3 and VEGF4, the same reaction conditions were used but with an annealing temperature of 56°C. This reaction was cycled 32 times.

In vitro *cell growth assay*

Cells of each tumor cell line (1×10^4) were plated in triplicate in 2.5 ml of Eagle's minimal essential medium in 6-well tissue culture plates. The medium in each well was changed every 48 h until the cells reached confluency. The cells were collected and counted with a hemacytometer every 24 h. The number of doublings was calculated using the formula $N_n/N_i = 2^x$ or $x = \ln(N_n/N_i)$, where N_n is the number of cells collected at time point n, N_i is the number of cells originally plated at time 0, and x is the number of population doublings.

In vivo *tumor growth*

TC71-neo and clone 17 cells in mid-log-growth phase were harvested by trypsinization. Single-cell suspensions (2×10^6 cells in 0.1 ml PBS) were injected subcutaneously into the ventral side of 6-week-old NOD/SCID mice. The tumors were measured every 2–4 days with a caliper, and the diameters were recorded. Ten mice were used for each group. Tumor volume was calculated by the formula: $a^2b/2$, where a and b are the 2 maximum diameters.

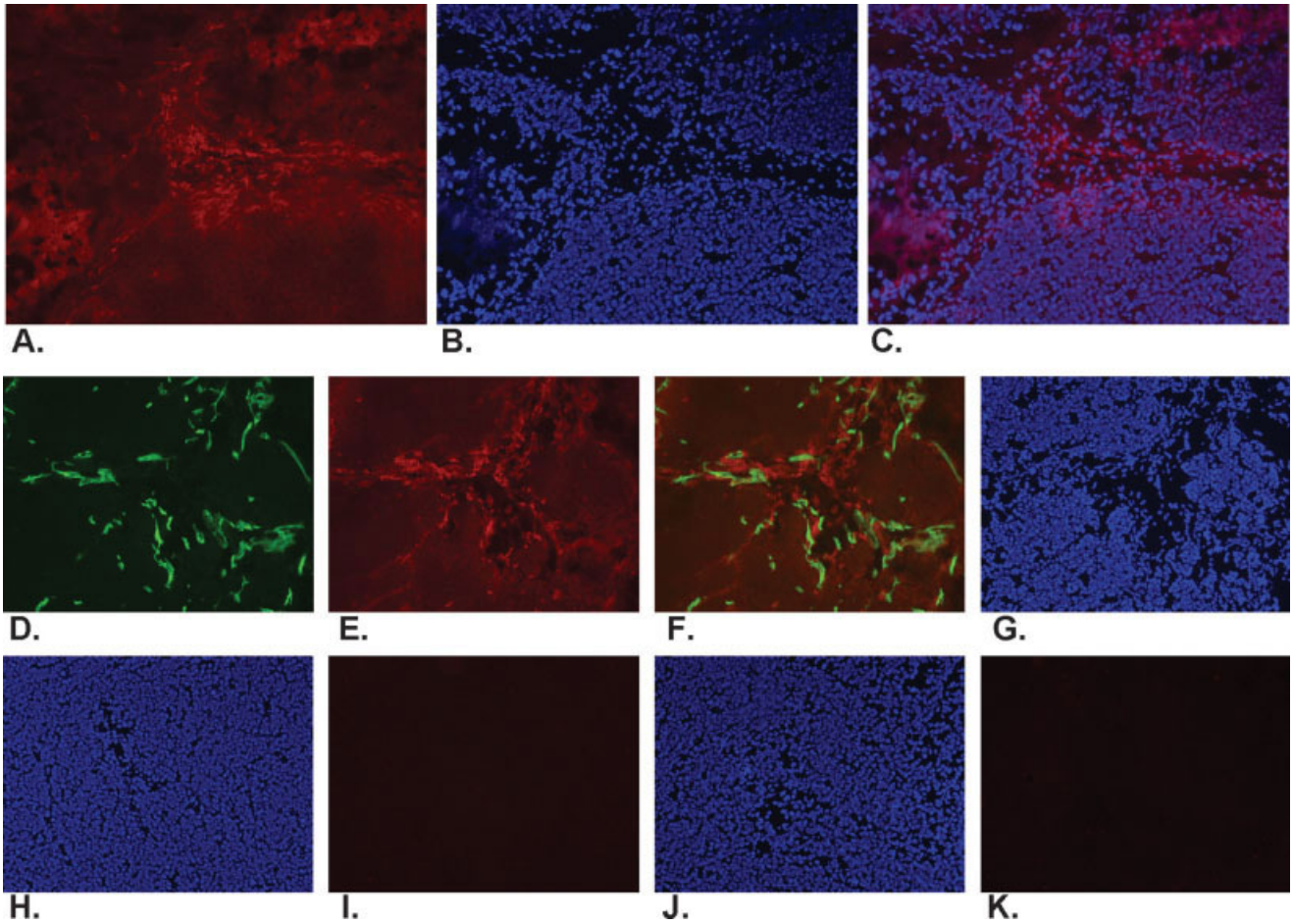

FIGURE 1 – Human CD34$^+$ cells migrate from the bone marrow to the tumor and incorporate into the tumor vasculature. (*a*) TC71 tumors from mice previously transplanted with human CD34$^+$ cells showed incorporation of human-derived VEC$^+$ cells (red) within the tumor area. (*b*) The same TC71 tumor area was stained with Hoescht 33342 dye to identify individual cells. When merged with the VEC image (*c*), positive staining for VEC showed that cells derived from the donor human CD34$^+$ cells migrated and incorporated into the tumor. Tumors taken from mice transplanted with CD34$^+$ cells were stained for mCD31 (*d*) and human VEC (*e*). The merged images (*f*) show human-derived cells in proximity to mouse vessels within the tumor. Hoescht 33342 staining (*g*) confirmed that the mCD31 and VEC expression was associated with cells. Hoescht 33342 staining of TC71 tumors taken from nontransplanted mice (*h*, *j*) revealed densely packed cells within the tumor area. There was no expression of human VEC (*i*, *k*) within these tumors, indicating no cross-reaction of the anti-VEC antibody with human tumor cells or mouse endothelial cells. Images were analyzed using a ×10 objective.

Statistical analysis

Two-tailed Wilcoxon matched-pairs signed rank test was used to statistically evaluate tumor volumes. Immunohistochemical staining was analyzed using single factor ANOVA. $p \leq 0.05$ was considered statistically significant.

Results

Migration of CD34$^+$ cells into TC71 Ewing's sarcoma tumors

Human CD34$^+$ cells were able to engraft and rescue sublethally irradiated mice (data not shown). We examined whether human CD34$^+$ cells migrate from the bone marrow into tumors. One week after transplantation with CD34$^+$ stem cells, SCID mice were subcutaneously injected with TC71 parental tumor cells. Two weeks later, the mice were killed and the tumors excised and sectioned. Microvessels were detected by immunohistochemical staining for mCD31, a marker for mouse endothelial cells. The sections were also immunostained for human VEC, an adhesion protein exclusively expressed on human vascular endothelial cells. TC71 tumors from mice transplanted with CD34$^+$ cells showed substantial incorporation of VEC$^+$ cells (Figs. 1*a*–1*c*).

Sections were costained for both mCD31 and VEC to determine the location of the human-derived cells within the tumors relative to the mouse microvessels. Costaining revealed many areas within the tumor where VEC$^+$ cells were in proximity to mCD31$^+$ microvessels (Figs. 1*d*–1*g*), suggesting that the human-derived VEC$^+$ cells participated in the expansion of the tumor vasculature. Superimposition of the mCD31 and VEC images did not reveal colocalization of the 2 markers on any cells. Colocalization would result in a yellow fluorescence in the merged image. This observation argues against cross-reaction of the mCD31 antibody with the human VEC antibody. It also argues against coexpression of both the mCD31 and VEC markers on the same cell that would indicate fusion of the human stem cells with mouse cells. No VEC$^+$ cells were detected in the tumors from mice that had not been transplanted with CD34$^+$ cells (Figs. 1*h*–1*k*).

To further analyze the relationship between CD34$^+$ cells and tumor vessels, the tumor sections were costained for mCD31 and VEC and analyzed by confocal microscopy. The tumor vessels were positive for both mCD31 and VEC staining (Fig. 2). The fluorescent signals were distinct for the Alexa 488 or Alexa 594 fluorophore, indicating that human cells and mouse cells were adjacent to each other. As seen in Figures 2*a* and 2*b*,

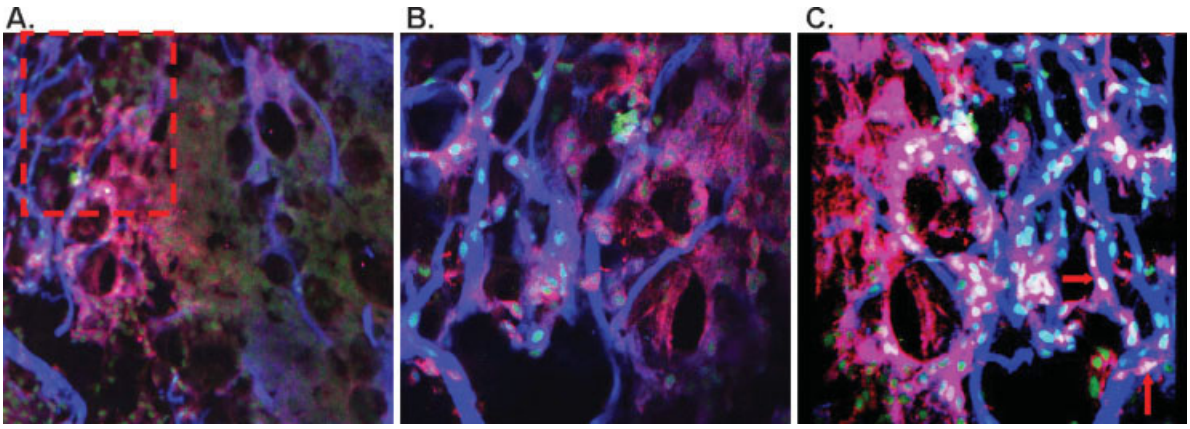

FIGURE 2 – Confocal microscopy of TC71 tumors from mice transplanted with $CD34^+$ cells. Tumor sections from transplanted mice were stained for mCD31 and human VEC. Green, cell nuclei; blue, mCD31; red, human VEC. (*a*) Numerous mouse vessels (blue) permeated the tumor (green), with discrete human VEC^+ cell clusters appearing close to mouse vessels. The area was analyzed with a ×10 objective. (*b*) The area enclosed by the dashed red box in (*a*) was analyzed with a ×40 objective. Human cells were observed immediately adjacent to mouse vessels. When the image was rotated 90° counterclockwise (*c*), human cells (red arrows) were seen wrapping around the outside of the mouse vessels (red arrows).

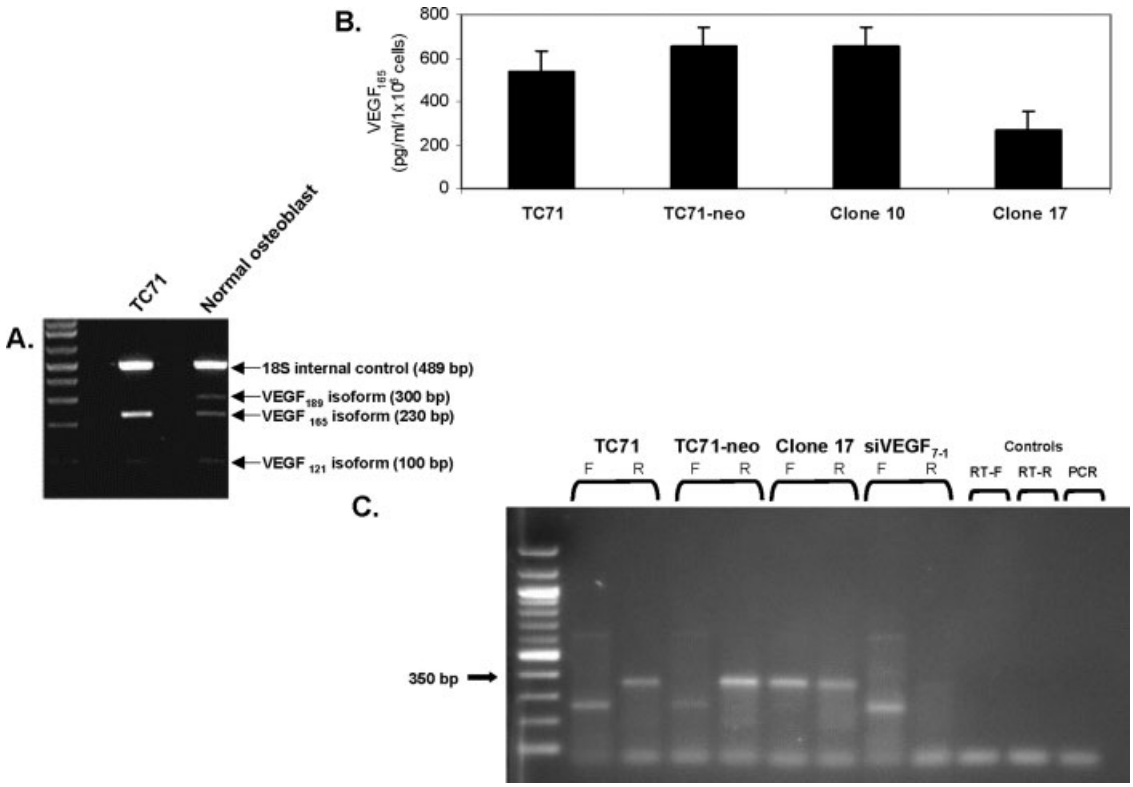

FIGURE 3 – VEGF expression and protein production in parental and $VEGF_{165}$-deficient transfected clones. (*a*) RT-PCR analysis of $VEGF_{121}$, $VEGF_{165}$, and $VEGF_{189}$. (*b*) Mean $VEGF_{165}$ production by TC71 parental cells, TC71-neo control cells, and the $VEGF_{165}$ antisense-transfected clones 10 and 17. Clone 17 had a 50% reduction in $VEGF_{165}$ protein production. (*c*) Strand-specific RT-PCR analysis of mRNA from TC71 parental, TC71-neo clone 17, and $siVEGF_{7\text{-}1}$ cells. 'F' and 'R' indicate whether forward or reverse DNA primers were used in the reverse transcriptase (RT) reaction to specifically amplify either the antisense or the sense strand of mRNA, respectively. The antisense $VEGF_{165}$ transcript (arrow) appears only in clone 17.

areas within the TC71 tumor contained dense clusters of VEC^+ cells that appeared to wrap around the mouse microvessels (Fig. 2*c*, red arrows). There were also areas that stained separately for either mCD31 or VEC.

The livers and spleens of $CD34^+$-transplanted mice were analyzed for incorporation of human-derived cells. The liver sections lacked any positive staining for HLA-A, HLA-B, or HLA-C, whereas the spleen had infrequent staining in small areas, indicating some infiltration into the organ (data not shown).

Migration of $CD34^+$ cells into Matrigel plugs containing recombinant human $VEGF_{165}$

Ewing's sarcoma cell lines overexpress VEGF compared to normal human osteoblasts,[15] with a shift in isoforms from $VEGF_{189}$

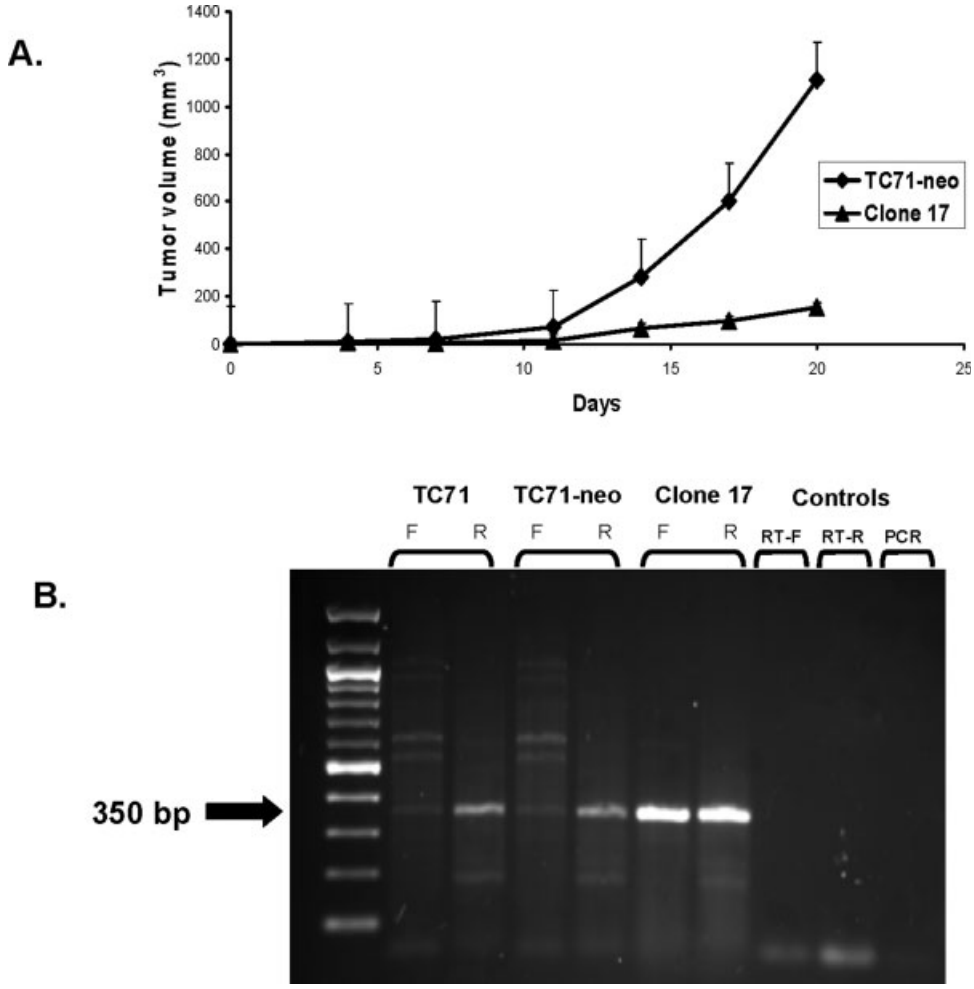

FIGURE 4 – Transfection of TC71 cells with antisense $VEGF_{165}$ reduces tumor growth *in vivo*. (*a*) Clone 17 cells grew more slowly *in vivo* compared to TC71-neo control cells ($p = 0.03$). Error bars indicate standard error. (*b*) TC71 parental, control-transfected (TC71-neo), and clone 17 cells were injected subcutaneously into NOD/SCID mice. Tumors were excised 2 weeks later. Strand-specific RT-PCR analysis revealed that expression of the antisense $VEGF_{165}$ transcript (arrow) was retained in the clone 17 tumor. F, forward primer; R, reverse primer.

to $VEGF_{165}$ (Fig. 3*a*). Since $VEGF_{165}$ has been shown to be a chemoattractant for $CD34^+$ cells, we examined whether $VEGF_{165}$ had a role in the migration of bone marrow cells to the growing Ewing's sarcoma tumor. One week after $CD34^+$ stem cell transplantation, SCID mice were subcutaneously implanted with Matrigel containing 200 ng/ml recombinant human $VEGF_{165}$. Two weeks later, the mice were killed and the Matrigel plugs excised. Immunohistochemical analysis showed that cells positive for human HLA-N20 were present within the Matrigel plugs containing $VEGF_{165}$ but not in the control Matrigel plugs (data not shown).

Characterization of antisense $VEGF_{165}$ TC71 clone

The antisense $VEGF_{165}$ clone 17 was constructed by transfecting TC71 Ewing's sarcoma cells with an antisense $VEGF_{165}$. Clone 17 showed a 50% reduction in VEGF production, as quantified by ELISA, compared to TC71 parental, TC71-neo vector control, and clone 10, a neomycin-resistant clone that demonstrated normal VEGF expression (Fig. 3*b*). Expression of antisense $VEGF_{165}$ mRNA was confirmed by strand-specific RT-PCR using the total mRNA isolated from TC71 parental, clone 17, and TC71-neo cells (Fig. 3*c*). DNA primers specific for either the sense or the antisense strands of $VEGF_{165}$ mRNA were used to prime the reverse transcriptase reaction. Subsequent PCR analysis of the first-strand cDNA demonstrated that only the clone 17 cells expressed the antisense $VEGF_{165}$ mRNA, whereas TC71 parental and TC71-neo cells expressed only endogenous sense $VEGF_{165}$ mRNA. The reduction in $VEGF_{165}$ protein production and the confirmation of antisense $VEGF_{165}$ mRNA expression confirmed the stable integration of the antisense $VEGF_{165}$ plasmid construct in the clone 17 cells.

The *in vitro* growth rate of clone 17 cells was analyzed by comparing the doubling time of these cells with that of the TC71 parental and TC71-neo cells. Doubling times for TC71 parental, TC71-neo, and clone 17 cells were all between 23 and 26 h, indicating that the *in vitro* proliferation rate of the clone 17 cells was comparable to that of the parental and vector control cells (data not shown) and was not affected by the transfection procedure or by the inhibition of $VEGF_{165}$. By contrast, the *in vivo* growth rate of clone 17 cells was significantly ($p = 0.03$) impaired compared to that of TC71-neo control tumors (Fig. 4*a*). Strand-specific RT-PCR confirmed that the clone 17 tumors retained expression of the antisense $VEGF_{165}$ transcript after 2 weeks of growth *in vivo* (Fig. 4*b*).

Migration of $CD34^+$ cells into $VEGF_{165}$-deficient TC71 tumors

Two $VEGF_{165}$-deficient TC71 Ewing's sarcoma cell lines were used to investigate the role of $VEGF_{165}$ in the migration of $CD34^+$ cells to the tumor area. In addition to clone 17, we used a small interfering $VEGF_{165}$ RNA (siRNA)-inhibited clone ($TC/siVEGF_{7\text{-}1}$)[22] (Fig. 3*c*) that was developed in our laboratory. $TC/siVEGF_{7\text{-}1}$ cells have a >90% reduction in $VEGF_{165}$ expression and VEGF protein production compared to that in TC71 parental cells and TC/si^- cells transfected with control siRNA.[22] Similar to clone 17 tumors, the $TC/siVEGF_{7\text{-}1}$ tumors had a significantly ($p < 0.01$) slower growth rate than that of TC71 parental and TC/si^- control tumors.[22]

TC71 parental, clone 17, TC71-neo, $TC/siVEGF_{7\text{-}1}$, and TC/si^- tumor cells were injected subcutaneously into SCID mice that had been previously transplanted with human $CD34^+$ stem cells. The

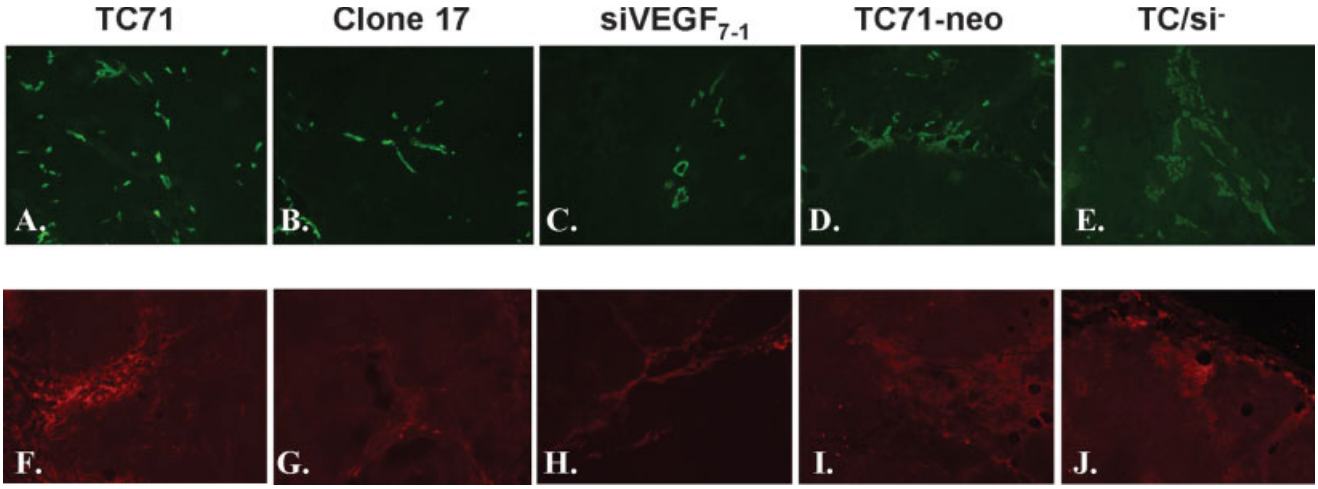

FIGURE 5 – Immunohistochemical analysis of mCD31 (top row, *a–e*) and human VEC (bottom row, *f–j*) tumors excised from mice previously transplanted with human $CD34^+$ cells and injected with TC71 (*a*,*f*), clone 17 (*b*, *g*), TC/siVEGF$_{7\text{-}1}$ (*c*, *h*), TC71-neo (*d*, *i*), or TC/si^- cells (*e*, *j*).

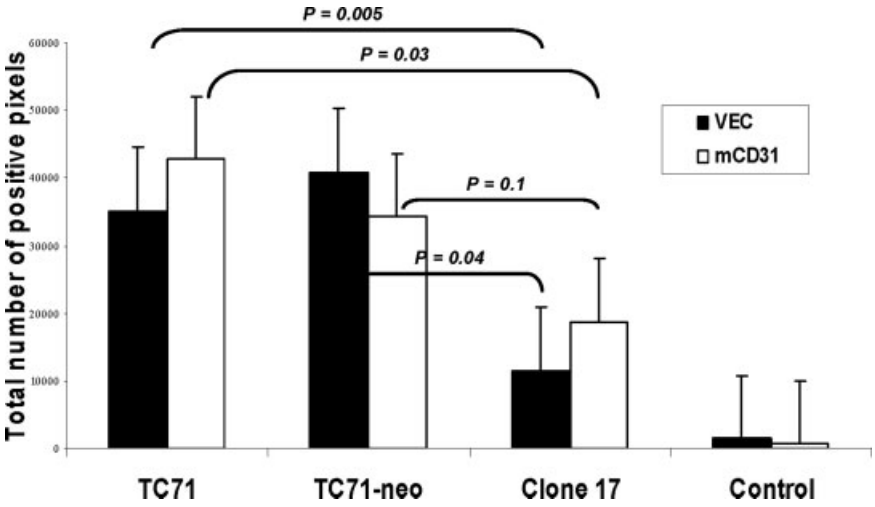

FIGURE 6 – Suppression of VEGF$_{165}$ reduces tumor vessel density and stem cell migration. SCID mice were transplanted with $CD34^+$ cells then subcutaneously injected with Matrigel containing the indicated tumor cells. As an additional negative control, one group of transplanted animals was implanted with Matrigel alone (control). Expression of human VEC and mCD31 was quantified by counting the total number of positive pixels per viewing field using a $\times 10$ objective. The data shown represent the mean $\pm$ S.E. from all viewing fields for each implant.

tumors were excised 2 weeks later. Fluorescent immunostaining revealed a decrease in vessels, as quantified by mCD31 staining, in both types of VEGF$_{165}$-deficient tumors (clone 17 and TC/siVEGF$_{7\text{-}1}$) compared to parental TC71, TC71-neo, and TC/si^- tumors (Figs. 5*a*–5*e*). Infiltration of transplanted human-derived cells was also substantially less in the clone 17 and TC/siVEGF$_{7\text{-}1}$ tumors (Figs. 5*g* and 5*h*) compared with the parental TC71, TC71-neo and TC/si^- control tumors (Figs. 5*f,* 5*i,* and 5*j*). Clone 17 tumors had some VEC^+ cells (Fig. 5*g*) but significantly fewer ($p < 0.05$) than did the TC71 and TC71-neo control tumors (Fig. 6). A statistically significant decrease in tumor vessels ($p = 0.03$) was also demonstrated between clone 17 tumors and TC71 tumors (Fig. 6). Although there were also fewer vessels in the clone 17 tumors compared to those in TC71-neo control tumors, this was not statistically significant ($p = 0.1$, Fig. 6).

The TC/siVEGF$_{7\text{-}1}$ tumors showed a greater reduction in *mCD31* staining within the tumor when compared with the clone 17 tumors (Fig. 5). This result is consistent with the greater reduction in VEGF$_{165}$ in the TC/siVEGF$_{7\text{-}1}$ cell line compared with that of clone 17 (90% versus 50%). The TC/siVEGF$_{7\text{-}1}$ tumors grew very slowly and were substantially smaller, with large necrotic centers, and so intact tumor cells were observed only as thin lines of cells covering the outside of the tumor/Matrigel implants. As a result, there were insufficient nonnecrotic viewing fields in the 10 TC/siVEGF$_{7\text{-}1}$ tumors for a complete statistical analysis. By contrast, the TC/si^- control tumors showed little necrosis and were well-vascularized. Our findings of reduced vascularization and decreased migration of bone marrow-derived cells into the tumor area suggest that VEGF$_{165}$ has a role in the chemoattraction of stem cells to the tumor.

Discussion

Using a transplant model, we showed that $CD34^+$ cells migrate into growing Ewing's sarcoma tumors and participate in the formation of the tumor neovasculature. Transplanting NOD/SCID mice with human cord blood $CD34^+$ cells allowed us to distinguish the bone marrow-derived cells from the local mouse endothelial cells. We demonstrated that human $CD34^+$ cells were able to rescue sublethally irradiated mice. Human derived cells were observed in the bone marrow and spleen, indicating engraftment. When Ewing's sarcoma cells were subcutaneously injected into $CD34^+$-transplanted mice, numerous human VEC^+ cells were found in the growing tumors 3 weeks later. Nontransplanted mice were devoid of human VEC^+ cells, indicating that the anti-human VEC-antibody was not cross-reactive with mouse cells or human Ewing's sarcoma cells. Together, these data indicate that the human cells in the tumor were derived from the $CD34^+$ stem cells.

The relationship between the human $CD34^+$-derived cells and the tumor microvessels was analyzed by staining for mCD31 and human VEC. Many areas within the tumors had VEC^+ cells in proximity to mouse endothelial cells (Fig. 1). Three-dimensional analysis using confocal fluorescence microscopy allowed a more detailed analysis of the positioning of the human cells in relation to the mouse endothelial cells. These confocal images demonstrated that the human VEC^+ cells were clustered and wrapped around the outside of the mouse microvessels (Fig. 2). These findings suggest an auxiliary or supportive role for the migrated human cells. We did not observe a mosaic pattern of human and mouse cells adjacent to each other forming a functional capillary tube. These observations warrant further investigation into the possible alternate development of the donor human $CD34^+$ cells into pericytes. The formation of pericytes have been shown to be crucial in early angiogenic development.[23] Thus, we are interested in also identifying the existence of human-derived pericytes developing in direct relation to host mouse-derived vessels and pericytes within the growing Ewing's tumor. Current staining techniques to identify pericytes markers are not optimal in distinguishing between human and mouse-derived cells. Some possible methods to address this issue include transplantation of mice with GFP-expressing human $CD34^+$ cells or transplanting female mice with male donor $CD34^+$ cells. Conclusive methods of identifying human and mouse pericytes or endothelial cells is necessary and will clarify whether these migrated cells have an essential role in the formation, growth, and remodeling of the tumor vessels. TC71 Ewing's sarcoma cells overexpress $VEGF_{165}$[15] which has chemotactic activity for endothelial progenitor cells.[24] $CD34^+$ cells express VEGF receptors 1 and 2 and are capable of differentiating into endothelial cells.[19,25] Our data show that the migration of $CD34^+$ cells to the tumor is dependent on tumor-derived $VEGF_{165}$. Specific reduction of the $VEGF_{165}$ isoform using either siRNA or antisense technology resulted in decreased recruitment of distal progenitor cells. The $VEGF_{165}$-deficient TC71 Ewing's tumors (clone 17 and TC/si$VEGF_{7\text{-}1}$) had significantly fewer VEC^+ cells compared with the control-transfected tumors (Figs. 5 and 6). The number of tumor vessels within the clone 17 and TC/si$VEGF_{7\text{-}1}$ tumors was also substantially decreased, and these vessels were less chaotic. These observations indicate that tumor-derived $VEGF_{165}$ may promote poorly formed and leaky vessels, consistent with the findings of others.[26,27]

Our data suggest that $VEGF_{165}$ production affects the distal mobilization and recruitment of bone marrow-derived $CD34^+$ stem cells into the tumor. Once in the tumor area, the $CD34^+$-derived cells support the tumor neovasculature, but it is not known whether these bone marrow-derived cells are crucial to the function and formation of the tumor vessels. The proximity of these cells to the mouse vessels suggests a cooperative role, but it does not definitively demonstrate that these cells are essential to the growth of the tumor or to the expansion of its vascular network to support tumor growth. It is also not clear whether bone marrow cells are more important in the early establishment of the tumor or whether the migration of stem cells is required even when the tumor is large and has a well-established vasculature. Determining the temporal dependence of Ewing's sarcoma on the recruitment of bone marrow cells will increase our understanding of the biology of this tumor. The identification of clusters of human-derived endothelial cells or pericytes in early tumors would suggest a significant role of bone marrow-derived cells in the initiation and early development of Ewing's tumors.[23] This understanding may in turn aid in the identification of new therapeutic approaches that target these progenitor cells to control or arrest tumor growth or exploit these cells as tumor-specific gene-delivery vehicles. The findings presented here, in addition to our previous investigations,[20] further document that vasculogenesis and angiogenesis may be involved in the growth and development of Ewing's sarcoma.

References

1. Burchill SA. Ewing's sarcoma: diagnostic, prognostic, and therapeutic implications of molecular abnormalities. J Clin Pathol 2003;56: 96–102.
2. Meyers PA, Levy AS. Ewing's sarcoma. Curr Treat Options Oncol 2000;1:247–57.
3. Delattre O, Zucman J, Melot T, Garau XS, Zucker JM, Lenoir GM, Ambros PF, Sheer D, Turc-Carel C, Triche TJ, Aurias A, Thomas G. The Ewing family of tumors—a subgroup of small-round-cell tumors defined by specific chimeric transcripts. N Engl J Med 1994; 331:294–9.
4. Grier HE. The Ewing family of tumors. Ewing's sarcoma and primitive neuroectodermal tumors. Pediatr Clin North Am 1997;44: 991–1004.
5. Pepper MS, Ferrara N, Orci L, Montesano R. Potent synergism between vascular endothelial growth factor and basic fibroblast growth factor in the induction of angiogenesis in vitro. Biochem Biophys Res Commun 1992;189:824–31.
6. Kliche S, Waltenberger J. VEGF receptor signaling and endothelial function. IUBMB Life 2001;52:61–6.
7. Senger DR, Van de Water L, Brown LF, Nagy JA, Yeo KT, Yeo TK, Berse B, Jackman RW, Dvorak AM, Dvorak HF. Vascular permeability factor (VPF, VEGF) in tumor biology. Cancer Metastasis Rev 1993;12:303–24.
8. Dvorak HF, Sioussat TM, Brown LF, Berse B, Nagy JA, Sotrel A, Manseau EJ, Van de Water L, Senger DR. Distribution of vascular permeability factor (vascular endothelial growth factor) in tumors: concentration in tumor blood vessels. J Exp Med 1991;174:1275–8.
9. Dvorak HF, Brown LF, Detmar M, Dvorak AM. Vascular permeability factor/vascular endothelial growth factor, microvascular hyperpermeability, and angiogenesis. Am J Pathol 1995;146:1029–39.
10. Hazelton D, Nicosia ,RF, Nicosia SV. Vascular endothelial growth factor levels in ovarian cyst fluid correlate with malignancy. Clin Cancer Res 1999;5:823–9.
11. Adams J, Carder PJ, Downey S, Forbes MA, MacLennan K, Allgar V, Kaufman S, Hallam S, Bicknell R, Walker JJ, Cairnduff F, Selby PJ, et al. Vascular endothelial growth factor (VEGF) in breast cancer: comparison of plasma, serum, and tissue VEGF and microvessel density and effects of tamoxifen. Cancer Res 2000;60:2898–905.
12. Cheng SY, Huang HJ, Nagane M, Ji XD, Wang D, Shih CC, Arap W, Huang CM, Cavenee WK. Suppression of glioblastoma angiogenicity and tumorigenicity by inhibition of endogenous expression of vascular endothelial growth factor. Proc Natl Acad Sci USA 1996;93: 8502–7.
13. Shaheen RM, Davis DW, Liu W, Zebrowski BK, Wilson MR, Bucana CD, McConkey DJ, McMahon G, Ellis LM. Antiangiogenic therapy targeting the tyrosine kinase receptor for vascular endothelial growth factor receptor inhibits the growth of colon cancer liver metastasis and induces tumor and endothelial cell apoptosis. Cancer Res 1999; 59:5412–6.
14. Yano S, Shinohara H, Herbst RS, Kuniyasu H, Bucana CD, Ellis LM, Davis DW, McConkey DJ, Fidler IJ. Expression of vascular endothelial growth factor is necessary but not sufficient for production and growth of brain metastasis. Cancer Res 2000;60:4959–67.
15. Zhou Z, Zhou RR, Guan H, Bucana CD, Kleinerman ES. E1A gene therapy inhibits angiogenesis in a Ewing's sarcoma animal model. Mol Cancer Ther 2003;2:1313–9.
16. Fuchs B, Inwards CY, Janknecht R. Vascular endothelial growth factor expression is up-regulated by EWS-ETS oncoproteins and Sp1 and may represent an independent predictor of survival in Ewing's sarcoma. Clin Cancer Res 2004;10:1344–53.
17. Asahara T, Takahashi T, Masuda H, Kalka C, Chen D, Iwaguro H, Inai Y, Silver M, Isner JM. VEGF contributes to postnatal neovascularization by mobilizing bone marrow-derived endothelial progenitor cells. Embo J 1999;18:3964–72.
18. Asahara T, Masuda H, Takahashi T, Kalka C, Pastore C, Silver M, Kearne M, Magner M, Isner JM. Bone marrow origin of endothelial progenitor cells responsible for postnatal vasculogenesis in physiological and pathological neovascularization. Circ Res 1999; 85:221–8.
19. Asahara T, Murohara T, Sullivan A, Silver M, van der Zee R, Li T, Witzenbichler B, Schatteman G, Isner JM. Isolation of putative progenitor endothelial cells for angiogenesis. Science 1997;275: 964–7.
20. Bolontrade MF, Zhou RR, Kleinerman ES. Vasculogenesis plays a role in the growth of ewing's sarcoma *in vivo*. Clin Cancer Res 2002; 8:3622–7.

21. Hogan CJ, Shpall EJ, McNulty O, McNiece I, Dick JE, Shultz LD, Keller G. Engraftment and development of human CD34(+)-enriched cells from umbilical cord blood in NOD/LtSz-scid/scid mice. Blood 1997;90:85–96.
22. Guan H, Zhou Z, Wang H, Jia SF, Liu W, Kleinerman ES. A small interfering RNA targeting vascular endothelial growth factor inhibits Ewing's sarcoma growth in a xenograft mouse model. Clin Cancer Res 2005;11:2662–9.
23. Ozerdem U, Stallcup WB. Early contribution of pericytes to angiogenic sprouting and tube formation. Angiogenesis 2003;6:241–9.
24. Young MR, Kolesiak K, Wright MA, Gabrilovich DI. Chemoattraction of femoral $CD34^+$ progenitor cells by tumor-derived vascular endothelial cell growth factor. Clin Exp Metastasis 1999;17:881–8.
25. Shi Q, Rafii S, Wu MH, Wijelath ES, Yu C, Ishida A, Fujita Y, Kothari S, Mohle R, Sauvage LR, Moore MA, Storb RF, et al. Evidence for circulating bone marrow-derived endothelial cells. Blood 1998;92:362–7.
26. Hashizume H, Baluk P, Morikawa S, McLean JW, Thurston G, Roberge S, Jain RK, McDonald DM. Openings between defective endothelial cells explain tumor vessel leakiness. Am J Pathol 2000;156:1363–80.
27. Carmeliet P, Jain RK. Angiogenesis in cancer and other diseases. Nature 2000;407:249–57.